INTERNATIONAL JOURNAL FOR NUMERICAL METHODS IN FLUIDS
Int. J. Numer. Meth. Fluids 2002; **39**:517–531 (DOI: 10.1002/fld.342)

Design optimization of axial flow hydraulic turbine runner: Part I—an improved Q3D inverse method

Guoyi Peng[1,*,†], Shuliang Cao[2], Masaru Ishizuka[1] and Shinji Hayama[1]

[1]*Department of Mechanical Systems Engineering, Faculty of Engineering, Toyama Prefectural University, 5180 Kurukawa, Kosugi-machi, Imizu-gun, Toyama 939-0398 Japan*
[2]*Department of Thermal Engineering, Tsinghua University, Beijing 100084, China*

SUMMARY

With the aim of constructing a comprehensive design optimization procedure of axial flow hydraulic turbine, an improved quasi-three-dimensional inverse method has been proposed from the viewpoint of system and a set of rotational flow governing equations as well as a blade geometry design equation has been derived. The computation domain is firstly taken from the inlet of guide vane to the far outlet of runner blade in the inverse method and flows in different regions are solved simultaneously. So the influence of wicket gate parameters on the runner blade design can be considered and the difficulty to define the flow condition at the runner blade inlet is surmounted. As a pre-computation of initial blade design on S_{2m} surface is newly adopted, the iteration of S_1 and S_{2m} surfaces has been reduced greatly and the convergence of inverse computation has been improved. The present model has been applied to the inverse computation of a Kaplan turbine runner. Experimental results and the direct flow analysis have proved the validation of inverse computation. Numerical investigations show that a proper enlargement of guide vane distribution diameter is advantageous to improve the performance of axial hydraulic turbine runner. Copyright © 2002 John Wiley & Sons, Ltd.

KEY WORDS: fluid machinery; hydraulic turbine; inverse problem; blade geometry design; computational fluid dynamics

1. INTRODUCTION

This paper is related to the inverse design optimization of axial flow hydraulic turbine runner. As the development of computational fluid dynamics, it becomes possible to analyse the complex internal flow in hydraulic machinery by solving the Navier–Stokes equations or [1] the three-dimensional (3D) Euler equations [2]. Compared with the direct problem of flow analysis, the inverse problem of blade geometry design is much more difficult. Nearly all inverse models are basically based on the inviscid assumption and some very useful simplified design methods have been developed with effort [3]. Concerning the inverse design of

* Correspondence to: Guoyi Peng, Department of Mechanical Systems Engineering, Faculty of Engineering, Toyama Prefectural University, 5180 Kurokawa, Kosugi-machi, Imizu-gun, Toyama 939-0398, Japan.
† E-mail: peng@pu-toyama.ac.jp

Received April 2001
Revised December 2001

turbo-machinery, especially hydraulic machinery runner blades, a survey of published literature indicates that only a few real 3D inverse models, such as the Fourier series expansion singularity method [4, 5], the pseudo-stream function method [6] and the inverse time marching method [7] have been reported. The pseudo-stream function method and the inverse time marching method are really an alteration of direct calculation and blade geometry modification. For the difficulty of defining a good relation between design specification and blade geometry modification, these two methods are very time consuming and further effort is needed to put them into practice applications. The Fourier expansion singularity method is originally developed for potential flow and then developed for rotational flow by Zangeneh *et al.* [8]. Although it can be applied to the inverse computation of axial flow hydraulic turbine runner [9], much effort is needed in order to obtain blade geometry of convergence near the tip where the swirl velocity has a great gradient in the radial direction due to the geometry of flow passage. Thus, much computation time will be taken when a Fourier expansion of many terms is adopted to improve the accuracy of inverse computation. Besides the above methods, some useful inverse methods are developed based on the general theory of two-type relative stream surfaces presented by Wu [10]. Similar to the computations of the Navier–Stokes equations and the Euler equations, a real three-dimensional iteration computation of S_1 (blade-to-blade) and S_2 (hub-to-shroud) surfaces is much time consuming. Therefore, a representative mean S_2 surface (S_{2m}) is usually introduced to reduce the iteration work. This is the so-called quasi-three-dimensional (Q3D) method. Compared to the fully three-dimensional computations, the Q3D inverse computation has a feature of quick convergence. Although the circumferential twist of S_1 surface is neglected, the Q3D inverse computation can provide a sufficient accuracy for engineering practice. Furthermore, with an accurate inverse model of quick convergence, it will become possible to find an optimum design plan by design optimization of comprehensive performance.

In the conventional Q3D inverse methods, the hydraulic turbine runner is usually treated as an isolated flow passing part. It is essential to define the flow boundary conditions at the upstream in front of the runner blade inlet and the downstream behind the blade outlet. These boundary conditions are usually defined empirically according to certain experimental data. In this way, the influence of wicket gate parameters on the inverse computation of runner blades cannot be taken into account [11]. In addition, it is difficult to find a universal runner blade inlet and outlet boundary conditions suitable for the flow computation of hydraulic turbine due to the limitation of the experiment. Especially, for the inverse problem, it is nearly impossible to define the flow conditions at inlet and outlet of runner blade according to experimental results because the blade shape is an unknown parameter to design.

On the above considerations, an improved Q3D method based on S_1 stream surfaces is proposed for axial hydraulic turbine runner design. First, in order to surmount the difficulty of defining flow conditions at blade inlet and outlet, the computation domain of inverse computation is taken from the far inlet of guide vane to the far outlet of runner blade. The flow in the range of guide vane and the flow in the bladeless region from the guide vane trailing edge to the blade inlet as well as the flow in the range of runner blade are computed simultaneously as a whole. So the influence of wicket gate parameters on the runner blade design can be taken into account through iteration computation. The difficulty of defining flow condition at blade inlet is surmounted. The second, a pre-computation of initial blade geometry on the mean S_{2m} surface is newly adopted in order to improve the convergence of inverse computation, and then the initial blade geometry is modified on S_1 surfaces. As the initial S_1 stream surfaces given through the pre-computation of initial blades on the S_{2m} surface are much close to the final ones, the iteration work of S_1 and S_{2m} surfaces is reduced and the convergence of inverse computation is much improved.

2. MATHEMATICAL MODEL

The real water flow in hydraulic turbines is viscous and weakly compressible. Cavitation will commence when the local static pressure is less than the vapour pressure of the water. Cavitation flow is highly compressible, and cavitations should be limited to a small area in a runner well designed even when they take place. Furthermore, avoiding cavitation should be one of the goals of runner blades design. Thus, the compressibility caused by cavitations is usually neglected in the inverse computation of hydraulic turbines. Instead, some efforts such as controlling of minimum local pressures are usually made to avoid cavitations. Concerning the fluid viscosity, on the one hand, experimental researches show that the effect of viscosity in hydraulic machinery is limited within a thin layer near the solid boundaries [1]. On the other hand, it is difficult to define a relation between design specification and blade geometry modification for the computation of Navier–Stokes equations [12]. Thus, the assumption of inviscid fluid is usually adopted in the inverse computation of hydraulic runner blade and the viscous flow separation and so on are controlled by defining certain constraints to the inverse design.

With the aim of constructing a practical comprehensive performance optimization procedure of hydraulic turbine [13], the present inverse model is also developed under the assumption of inviscid incompressible flow in order to obtain a quick convergence. The viscous effect is estimated through viscous flow analysis, and the flow separation is controlled by adjusting the values of design parameters through optimization procedure. The problem of cavitations is considered by defining a constraint that the local minimum static pressure is greater than the vapour pressure of water for the inversed design and finding a minimum value of cavitation coefficient through optimization of blade loading distribution.

In the present theory, the 3D internal flow of hydraulic turbine is calculated by iteration computations of the mean S_2 stream surface and a series of S_1 stream surfaces is based on the theory of two-type relative stream surfaces, and the governing equations of inverse computation is derived as follows.

2.1. Circumferentially averaged mean flow computation

Figure 1 shows the schematic configuration of axial flow hydraulic turbine to be researched. In a right-handed cylindrical polar co-ordinate system defined by (z, r, θ) which is rotating together with the impeller, the continuity and momentum equation of the three-dimensional rotational steady flow in hydraulic turbines is known to be as follows:

$$\nabla \cdot \mathbf{W} = 0 \tag{1}$$

$$\mathbf{W} \times (\nabla \times \mathbf{V}) = \nabla E_{\mathrm{r}} \tag{2}$$

in which

$$E_{\mathrm{r}} = \left(\frac{V^2}{2} + \frac{p}{\rho} + gz\right) - \omega V_\theta r$$

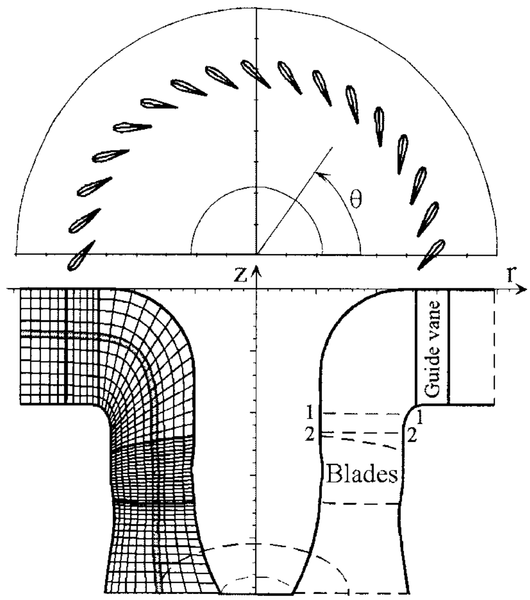

Figure 1. Scheme of Kaplan turbine and the meridional flow passage.

where E_r denotes the relative total enthalpy per unit mass. $\vec{W}$ and $\vec{V}$ denotes the relative velocity and absolute velocity, respectively. g denotes the gravity and z the axial co-ordinate. p and ρ represent the pressure and the density of working fluid, respectively. In order to derive the flow governing equation on the mean stream surface $S_{2\mathrm{m}}$, we define a circumferentially averaging operation as follows:

$$\bar{\mathbf{f}} = \frac{1}{\theta_\mathrm{p} - \theta_\mathrm{s}} \int_{\theta_\mathrm{s}}^{\theta_\mathrm{p}} \mathbf{f}(z, r, \theta)\,\mathrm{d}\theta \tag{3}$$

where $\vec{f}$ denotes an arbitrary physical quantity. θ_p and θ_s denote the angular co-ordinate of the pressure surface and the suction surface of two adjacent blades. Taking the circumferentially averaging operation to Equations (1) and (2), we obtain the following governing equations of the averaging mean flow:

$$\nabla \cdot [(\theta_\mathrm{p} - \theta_\mathrm{s})\overline{\mathbf{W}}] = 0 \tag{4}$$

$$\overline{\mathbf{W}} \times (\nabla \times \overline{\mathbf{V}}) + \mathbf{R} = -\mathbf{F}_\mathrm{b} + \nabla \bar{E}_\mathrm{r} \tag{5}$$

in which

$$\mathbf{F}_\mathrm{b} = \overline{\mathbf{W}} \times \frac{1}{(\theta_\mathrm{s} - \theta_\mathrm{p})H_\theta n_\theta} \Delta_\mathrm{ps}(\mathbf{n} \times \widetilde{\mathbf{W}}), \qquad \mathbf{R} = \overline{\widetilde{\mathbf{W}} \times (\nabla \times \widetilde{\mathbf{V}})}$$

$$\Delta_\mathrm{ps}(\mathbf{n} \times \widetilde{\mathbf{W}}) = (\mathbf{n} \times \widetilde{\mathbf{W}})|_{\theta=\theta_\mathrm{p}} - (\mathbf{n} \times \widetilde{\mathbf{W}})|_{\theta=\theta_\mathrm{s}}, \qquad \widetilde{\mathbf{W}} = \mathbf{W} - \overline{\mathbf{W}}, \quad \widetilde{\mathbf{V}} = \mathbf{V} - \overline{\mathbf{V}}$$

where $\mathbf{F}_b$ represents the action of blade to the mean flow and its direction lays in the direction of blade mean surface, that is $\mathbf{F}_b \times \mathbf{n} = 0$. $\mathbf{R}$ represents the effect of flow periodicity in the circumferential direction. It is a high order infinitesimal term caused by the circumferential flow variation due to the blade thickness and the finite number of blades [14] and is neglected in this computation. The subscript θ denotes the component in the circumferential direction. H denotes the Lame coefficients of co-ordinate scale factor, and they are given as $H_z = H_r = 1$ and $H_\theta = r$ in the cylindrical co-ordinate system (z, r, θ). The vector $\mathbf{n}$ denotes the normal unit of the circumferentially averaged mean flow surface S_{2m} that is thought to be parallel to the blade mean surface in the blade region. Thus, the normal unit vector can be given as follows:

$$\mathbf{n} = \frac{\nabla S}{|\nabla S|} \tag{6}$$

where S denotes the covert function of blade mean surfaces. In the (z, r, θ) co-ordinate system, the blade mean surfaces can be expressed as follows:

$$\begin{aligned} S(z,r,\theta) &= \theta - \varphi(z,r) \\ &= k\,\frac{2\pi}{N_b} \quad (k = 0, \pm 1, \pm 2, \ldots) \end{aligned} \tag{7}$$

where $\varphi(z,r)$ is the angular co-ordinate of blade mean surfaces and N_b is the number of runner blades. Taking into account Equation (6), we obtain the following expression:

$$\mathbf{n} = \frac{1}{\sqrt{1 + (r\partial\varphi/\partial r)^2 + (r\partial\varphi/\partial z)^2}} \left(\mathbf{e}_\theta - \frac{r\partial\varphi}{\partial r}\,\mathbf{e}_r - \frac{r\partial\varphi}{\partial z}\,\mathbf{e}_z \right) \tag{8}$$

where $\mathbf{e}$ denotes a unit vector and subscripts r, θ, z denote the direction of the corresponding co-ordinate, respectively. Multiplied by the unit normal of blade mean surface, Equation (5) can be written as follows:

$$\mathbf{n} \times [\overline{\mathbf{W}} \times (\nabla \times \overline{\mathbf{V}})] = \mathbf{n} \times \nabla \bar{E}_r \tag{9}$$

Arranging the above expression, we obtain the following equation of partial difference:

$$\begin{aligned} \frac{\partial \overline{W}_z}{\partial r} - \frac{\partial \overline{W}_r}{\partial z} &= \frac{\partial\varphi}{\partial r}\,\frac{\partial \bar{V}_\theta r}{\partial z} - \frac{\partial\varphi}{\partial z}\,\frac{\partial \bar{V}_\theta r}{\partial r} \\ &\quad + \frac{1}{\overline{W}^2}\left[\frac{\partial \bar{E}_r}{\partial r}\left(\overline{W}_r + \overline{W}_\theta\,\frac{r\partial\varphi}{\partial z} \right) - \frac{\partial \bar{E}_r}{\partial z}\left(\overline{W}_r + \overline{W}_\theta\,\frac{r\partial\varphi}{\partial r} \right) \right] \end{aligned} \tag{10}$$

where $\overline{W}^2 = \overline{W}_r^2 + \overline{W}_\theta^2 + \overline{W}_z^2$, $\bar{V}_\theta r$ is called the mean velocity torque (or mean swirl velocity), which is directly related to the mean blade bound circulation $\Gamma = 2\pi \bar{V}_\theta r$.

Concerning the conservation of mass, we define the following stream function from Equation (4).

$$\frac{\partial \Psi}{\partial r} = rB_f \overline{W}_z, \quad \frac{\partial \Psi}{\partial z} = -rB_f \overline{W}_r \tag{11}$$

where B_{f} denotes the blade blockage coefficient that is given as $B_{\mathrm{f}} = N_{\mathrm{b}}(\theta_{\mathrm{p}} - \theta_{\mathrm{s}})/2\pi$. Taking the stream function into Equation (10), we derive the following equation of stream function governing the circumferentially averaged mean flow:

$$\frac{\partial}{\partial r}\left(\frac{1}{rB_{\mathrm{f}}}\frac{\partial\Psi}{\partial r}\right) + \frac{\partial}{\partial z}\left(\frac{1}{rB_{\mathrm{f}}}\frac{\partial\Psi}{\partial z}\right) = \frac{\partial\varphi}{\partial r}\frac{\partial\bar{V}_\theta r}{\partial z} - \frac{\partial\varphi}{\partial z}\frac{\partial\bar{V}_\theta r}{\partial r} + \frac{1}{\overline{W}^2}\left[\frac{\partial E_{\mathrm{r}}}{\partial r}\left(\overline{W}_r + \overline{W}_\theta\frac{r\partial\varphi}{\partial z}\right) - \frac{\partial E_{\mathrm{r}}}{\partial z}\left(\overline{W}_r + \overline{W}_\theta\frac{r\partial\varphi}{\partial r}\right)\right] \tag{12}$$

This is a 2D elliptic partial difference equation. It should be solved subjected to boundary conditions at tip and hub end walls as well as the upstream and the downstream. At the upstream near the blade inlet, the inflow is influenced by the blade geometry to be designed. So, it is very difficult to define the flow condition near the blade inlet [15]. On the other hand, the flow at the far inlet of wicket gate is approximately uniform. It is convenient to give the flow condition there. In the view of systems, the flow in the region of guide vane and the flow through the runner are interrelated. It is more reasonable to deal with the flow from the inlet of guide vane to the outlet of runner blade. On this consideration, the computation domain of circumferentially averaged mean flow is firstly taken from the far inlet of guide vane to the fare outlet of runner blade in the present inverse computation. In this way, the difficulty to define flow condition at the upstream near the blade can be surmounted. Then, flow governing equations for the region of guide vane as well as bladeless regions in front and behind the runner are required to be added.

For the flow in the range of wicket gate, $\omega = 0$. According to the conservation of energy, we know that the absolute enthalpy per unit mass $E_i = V^2/2 + p/\rho + gz$ should be constant anywhere. Then the flow governing equation in the range of guide vane can be derived as follows from Equation (2) in the same way as above:

$$\frac{\partial}{\partial r}\left(\frac{1}{rB_{\mathrm{f}}}\frac{\partial\Psi}{\partial r}\right) + \frac{\partial}{\partial z}\left(\frac{1}{rB_{\mathrm{f}}}\frac{\partial\Psi}{\partial z}\right) = \frac{\partial\varphi}{\partial r}\frac{\partial\bar{V}_\theta r}{\partial z} - \frac{\partial\varphi}{\partial z}\frac{\partial\bar{V}_\theta r}{\partial r} \tag{13}$$

in which φ denotes the angular co-ordinate of the mean surface of guide vane and B_{f} its blockage coefficient.

In bladeless non-rotating regions, the equation of motion can be written as follows under the assumption of inviscid incompressible steady flow:

$$\mathbf{V} \times (\nabla \times \mathbf{V}) = 0 \tag{14}$$

Similarly, the following flow governing equation of stream function can be derived from above:

$$\frac{\partial}{\partial r}\left(\frac{1}{r}\frac{\partial\Psi}{\partial r}\right) + \frac{\partial}{\partial z}\left(\frac{1}{r}\frac{\partial\Psi}{\partial z}\right) = \frac{\bar{V}_\theta r}{\bar{V}_m^2 r^2}\left(\bar{V}_r\frac{\partial\bar{V}_\theta r}{\partial z} - \bar{V}_z\frac{\partial\bar{V}_\theta r}{\partial r}\right) \tag{15}$$

where $\bar{V}_m^2 = \bar{V}_r^2 + \bar{V}_z^2$.

As the right-hand side of Equation (12) includes the unknown parameter φ of blade geometry to be designed, the above set of equations should be solved simultaneously by iteration

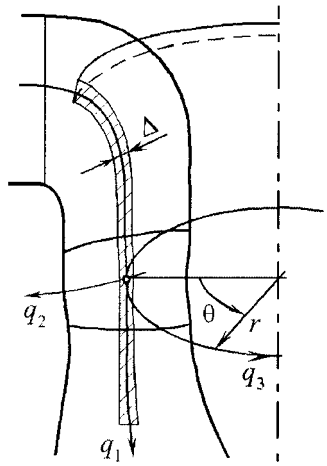

Figure 2. Curvilinear co-ordinates on the S_1 surface.

method. For the computation domain shown in Figure 1, boundary conditions are given as follows: (a) At end wall of hub streamline $\Psi = 0$. (b) At end wall of shroud streamline $\Psi = Q/2\pi$, where Q denotes the volumetric flow rate. (c) At the upstream, $\partial\Psi/\partial n = 0$. (d) At the downstream, $\Psi = \Psi_o(r)$, where $\Psi_o(r)$ is a distribution function affected by the geometry of flow path and the shape of blade [11, 16]. For the difficulty to define directly, the distribution function at runner exit is modified iteratively to keep a natural exit flow along S_1 stream surfaces.

2.2. *Governing equation on S_1 stream surfaces*

With regard to the actual practice of hydraulic machinery, S_1 stream surfaces relative to runner blades are twisted curved surfaces. For its twist in the circumferential direction is very small, S_1 stream surfaces are usually assumed to be symmetric in the engineering practice [17].

In order to derive the flow governing equation on S_1 surface, an orthogonal curvilinear co-ordinate system ($q_1 = m$, q_2, $q_3 = \theta$) shown in Figure 2 is adopted on S_1 stream surface, in which q_1 is in the direction of meridional streamline and $q_3 = r_0\theta$ in the circumferential direction. $\mathbf{q}_2 = \mathbf{q}_1 \times \mathbf{q}_3$ is the out normal direction of S_1 surface. r_0 denotes the radius of the co-ordinate origin. Then the Lame coefficient of the co-ordinates can be given as, $H_1 = 1$, $H_2 = h(q_1)$ $H_3 = r/r_0$, where $h(q_1)$ denotes the dimensionless thickness of S_1 stream layer normalized with the thickness at the co-ordinate origin. Under the assumption of circumferential uniform inflow, we know that the vorticity of absolute motion on the S_1 surface equals zero. That is, $\mathrm{rot}_2\,\mathbf{V} = 0$, which can be written as follows:

$$\frac{1}{H_1 H_3}\left(\frac{\partial(H_1 W_1)}{\partial q_3} - \frac{\partial(H_3 W_3)}{\partial q_1}\right) - 2\omega\frac{\partial r}{H_1 \partial q_1} = 0 \qquad (16)$$

Arranging the above expression, we obtain the following equation:

$$\frac{\partial W_m}{\partial\theta} - \frac{\partial(rW_\theta)}{\partial m} = 2\omega r\frac{\partial r}{\partial m} \qquad (17)$$

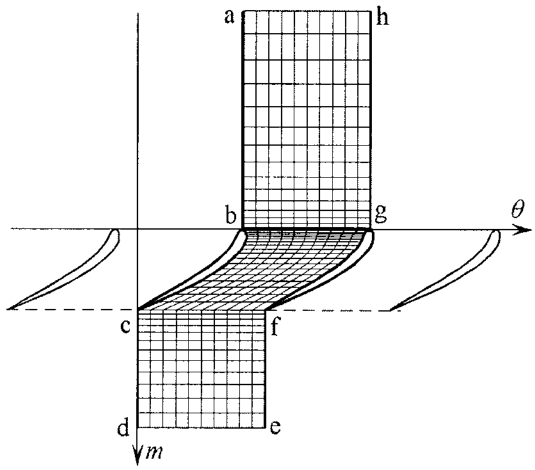

Figure 3. Expansion of S_1 stream surface.

As the co-ordinate q_2 is normal to the S_1 stream surface, its velocity component W_2 should be zero, the continuity of mass reduces to the following form:

$$\frac{\partial}{\partial q_1}(H_2 H_3 W_1) + \frac{\partial}{\partial q_3}(H_1 H_2 W_3) = 0 \tag{18}$$

This equation can be written as follows:

$$\frac{\partial}{\partial m}(hrW_m) + \frac{\partial}{\partial \theta}(hW_\theta) = 0 \tag{19}$$

Based on the above continuity equation, a stream function on the S_1 stream surface can be defined as

$$\frac{\partial \Psi}{\partial \theta} = hrW_m, \quad \frac{\partial \Psi}{\partial m} = -hW_\theta \tag{20}$$

Then, a general stream function equation governing the flow on S_1 stream surface is derived from Equation (17)

$$\frac{\partial}{\partial m}\left(\frac{r}{h}\frac{\partial \Psi}{\partial m}\right) + \frac{\partial}{\partial \theta}\left(\frac{1}{hr}\frac{\partial \Psi}{\partial \theta}\right) = 2\omega r\frac{\partial r}{\partial m} \tag{21}$$

This equation is the 2D one concerning m and θ. Thus, it is solved in the expand surface shown in Figure 3.

In solving the above equation, parameters $h(m)$ and $\partial r/\partial m$ should be defined through flow computation of the $S_{2\mathrm{m}}$ stream surface. The boundary conditions for the computation domain shown in Figure 3 are given as follows:

(a) At the upstream and the downstream, $\partial\Psi/\partial n|_{ah} = hW_\theta|_{ah}$, $\partial\Psi/\partial n|_{de} = hW_\theta|_{de}$.
(b) On blade suction and pressure surfaces, $\Psi|_{\mathrm{bc}} = 0$, $\Psi|_{fg} = \mathrm{d}q$, where $\mathrm{d}q$ is the partial flow rate passing through two adjacent blades on the stream surface.

(c) Periodic boundary conditions, $\Psi|_{ef} = \Psi|_{cd} + \mathrm{d}q$, $\psi|_{gh} = \psi|_{ab} + \mathrm{d}q$.
(d) The Kutta–Joukwski condition, $W_f = W_\mathrm{c}$

Concerning the Kutta–Joukwski boundary condition, the flow on S_1 surfaces is computed iteratively.

2.3. *Equation of blade geometry design*

Once the flow field is determined, it is possible to calculate the shape of the blade by imposing the inviscid slip boundary condition that the blade should be aligned with the local velocity vector. The condition can be expressed as

$$\mathbf{W}_\mathrm{b} \cdot \nabla S = 0 \tag{22}$$

where $\mathbf{W}_\mathrm{b}$ denotes the velocity at the blade mean surface and $\mathbf{W}_\mathrm{b} = (\mathbf{W}_\mathrm{p} + \mathbf{W}_\mathrm{s})/2$, in which $\mathbf{W}_\mathrm{p}$ and $\mathbf{W}_\mathrm{s}$ denote relative velocity vectors on pressure and suction surfaces of blade, respectively. According to Equation (6), we obtain the following equation:

$$W_{\mathrm{b},r} \frac{\partial \varphi}{\partial r} + W_{\mathrm{b},z} \frac{\partial \varphi}{\partial z} = \frac{1}{r^2} (\bar{V}_\theta r - \omega r^2) \tag{23}$$

Averaging the above equation circumferentially and arranging the expression, we obtain the following equation of blade mean surface computation:

$$\overline{W}_m r^2 \frac{\mathrm{d}\varphi}{\mathrm{d}m} = \bar{V}_\theta r - \omega r^2 \tag{24}$$

The above first-order differential equation can be easily solved by iteration. The integration, as in the case of other initial value problems, requires an initial condition. The initial condition, which is called stacking condition of blade design, is implemented as an input by giving the following relation here:

$$\varphi(z = z_\mathrm{st}, r, \theta) = \varphi_0 \tag{25}$$

where z_st and φ_0 denote the given co-ordinates of stacking axis. With the above blade stacking condition, Equation (24) is easily applied to design the shape of blade mean surface. For the computation of $S_{2\mathrm{m}}$ stream surface treats the three-dimensional flow as a circumferential uniform one, which is only suitable for a runner with the many thin blade, the blade designed on $S_{2\mathrm{m}}$ surface cannot guarantee the variation of swirl velocity. Especially for the axial flow hydraulic turbine runner with a few blades, it is necessary to modify the blade geometry on S_1 surfaces considering the circumferential flow variation. Thus, the following relax iteration formula of the mean blade surface based on $S_{2\mathrm{m}}$ surfaces is derived from Equation (24):

$$\varphi^{(n+1)} = \varphi^{(n)} + \lambda \int \frac{(\bar{V}_\theta r)^g - (\bar{V}_\theta r)^{(n)}}{W_m r^2} \, \mathrm{d}m \tag{26}$$

where λ denotes a relaxation coefficient. The superscript $n+1$ denotes the computation result of a new step and n the one of the previous step. $(\bar{V}_\theta r)^g$ is the given velocity torque distribution of design specification. After getting a new blade mean surface, new blade pressure and suction surfaces are calculated according to the blade thickness in the circumferential direction in the present computation. The circumferential thickness of blade can be computed using the following formula [18]:

$$t_\theta(z,r) = t_{\mathrm{n}}(z,r)\left[1 + r^2\left(\frac{\partial\varphi}{\partial r}\right)^2 + r^2\left(\frac{\partial\varphi}{\partial z}\right)^2\right]^{1/2} \tag{27}$$

where $t_{\mathrm{n}}(z,r)$ denotes the normal thickness distribution which is given as a design specification.

Summarizing the above statement, we know that the first step of the present Q3D inverse model is to design an initial blade through the inverse computation on the mean $S_{2\mathrm{m}}$ surface until convergence. Then, the next is to modify the blade geometry through iteration computations of the inverse problem on S_1 stream surfaces and the direct problem on $S_{2\mathrm{m}}$ stream surface. Compared to traditional Q3D methods of axial hydraulic turbine runner blade design where the blade geometry is directly calculated on S_1 surfaces given by meridional flow computation, the iteration numbers of S_1 and $S_{2\mathrm{m}}$ surfaces in the present improved method has been reduced greatly because a reasonable initial blade is calculated on $S_{2\mathrm{m}}$ surface and initial S_1 stream surfaces close to the final ones are defined considering the effect of initial blade geometry on $S_{2\mathrm{m}}$ surface.

3. NUMERICAL RESULTS

3.1. Experimental validation

As a numerical example, the present inverse model is applied to design a Kaplan turbine runner using a finite element method. Basic design parameters of the turbine model are given as: the specific speed $n_{\mathrm{s}} = 440\,\mathrm{mkW}$, the rotational speed of designing $n_{10} = 115\ \mathrm{min}^{-1}$, the volumetric flow rate $Q_{10} = 1.250\mathrm{m}^3/\,\mathrm{min}$, the diameter of the runner to be designed $D_1 = 1.0\mathrm{m}$, the working head $H = 1.0\ \mathrm{m}$, the number of blades $N_{\mathrm{b}} = 6$, the diameter of pitch circle for guide vane distribution $D_0 = 1.16D_1$, the height of guide vane (span length) $B_0 = 0.375D_1$.

The guide vane is chosen to be the standard symmetric one. The flow passage and computation domain is given as shown in Figure 1. In order to prove the validation of dealing with flows in different regions by the simultaneous combination computation method, the velocity distribution in the bladeless region from the guide vane trailing edge to the runner blade leading edge are investigated numerically and experimentally. Figure 4 shows the velocity distributions on Sections $1-1$ and $2-2$ given in Figure 1, where the solid line and the dashed line represent, respectively, the computational and the experimental results. The figure demonstrates that computational results coincide with experimental ones well. Thereby, the validation of the present simultaneous combination computation of different flow regions has been proved. The method of defining the flow boundary condition at the runner blade inlet by combination computation is reliable.

3.2. Inverse computation

The mean velocity torque distribution, $\bar{V}_\theta r$, is an important design specification that determines the runner blade geometry and thus have a great influence on the performance of the designed runner. For the hydraulic turbine runner, the value of velocity torque at the runner blade leading edge is determined by the inflow of upstream from guide vanes. The variation of

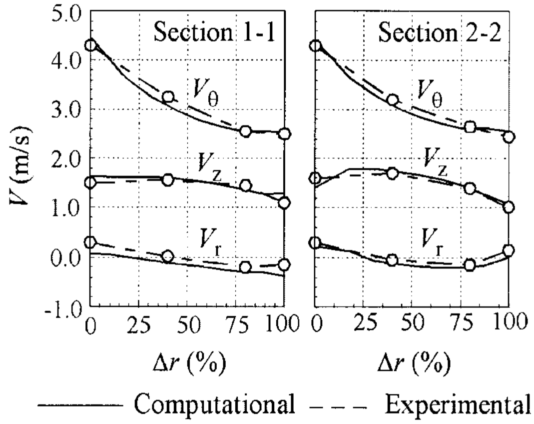

Figure 4. Comparison of computational results with experimental ones.

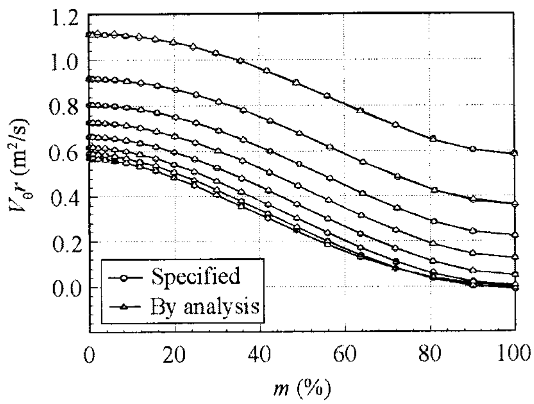

Figure 5. Velocity torque distribution along streamlines.

velocity torque from the blade leading edge to the trailing edge is determined by the blade duty of the designed runner obeying the conservation of energy. In order to satisfy the Kutta–Joukowsky condition, the derivation of velocity torque in the streamline direction should be set to zero at the blade leading edge. Considering the above points, we define the velocity torque distribution as a fourth polynomial in the stream direction from the blade leading edge to the trailing edge. Figure 5 shows the results of actually specified velocity torque distribution along streamlines from the blade leading edge to the trailing edge by circles. The blade normal thickness distribution along streamline is given as that of RAF-6 hydrofoil. Under the meridional geometry shown in Figure 1, runner blades have been designed using the computer code of the present inverse model. Figure 6 shows the geometry of designed blade on cylindrical sections uniformly taken from the hub to the tip. The figure demonstrates that the designed blade is smoothing and reasonable. Figure 7 shows the contour of velocity torque distribution in the blade region. From the figure we understand that the gradient of velocity torque in the radial direction is very large near the tip. So the flow through Kaplan

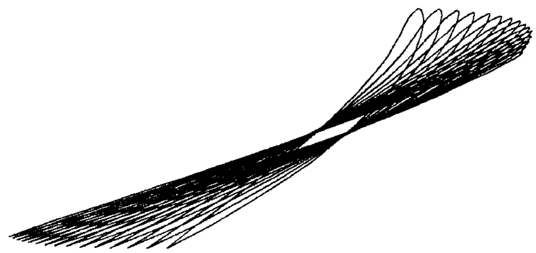

Figure 6. Designed blade geometry on cylindrical sections.

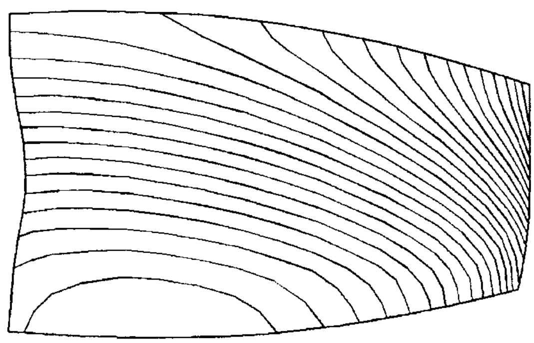

Figure 7. Contours of velocity torque in the blade region.

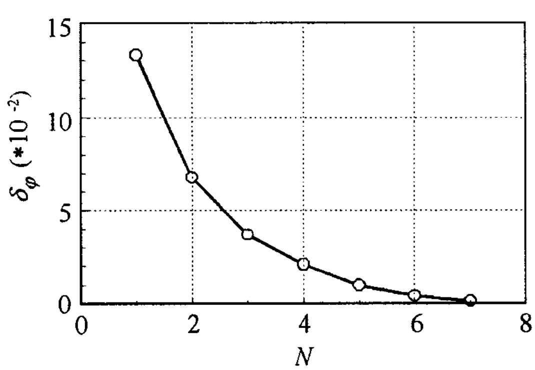

Figure 8. Convergence history of blade geometry design on S_1 surface.

runner is a rotational flow with large vorticity. This is the characteristic of the flow in axial flow hydraulic turbine different from other ones. Concerning the convergence of the present model, the iteration numbers between S_{2m} and S_1 surfaces is about 3–5, which is only about 1/3 of the case without the pre-computation of initial blade design on the S_{2m} surface. The computation time on a personal computer of 200 MHz is only about 5 min. Figure 8 shows the convergence history of blade geometry design on S_1 surfaces in which a good convergence property is demonstrated.

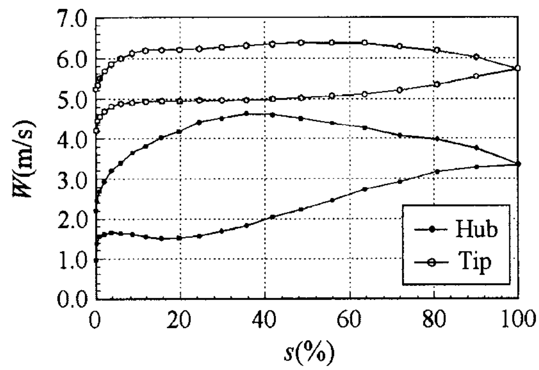

Figure 9. Relative velocity distribution on blade surfaces.

In the present inverse model, first, the influence of blade geometry on the mean flow is considered in the process of designing an initial blade on the S_{2m} surface. So the initial S_1 stream surfaces defined through the computation of S_{2m} surface are much more close to the final ones and then the iteration of S_1 surfaces and the S_{2m} surface is reduced greatly. Second, the circumferential flow variation is taken into account by modifying the blade geometry on S_1 stream surfaces. So the designed runner meets the output requirement quite well. The present Q3D inverse model is a simple and but an effective inverse design method fit for engineering practice.

In order to verify the validity of the inverse computation, the flow through the designed runner has been investigated by direct flow analysis. Figure 9 shows relative velocity distributions on the suction and pressure surfaces of hub and tip blade by dots and circles, respectively, in which s denotes the streamline co-ordinate on the mean blade surface. According to the result, we know that the designed runner blade geometry is reasonable. The velocity torque distributions along streamlines obtained by flow analysis of designed runner blades are shown in Figure 5 with triangles. The figure indicates that the velocity torque distribution of the designed runner coincides well with the design specification. This means that the designed runner blade meets the design requirement of output well.

3.3. Influence of wicket gate parameters on blade design

The height B_0 of guide vane and the diameter D_0 of guide vane distribution are the main parameters of wicket gates. According to the above inverse computation, these two parameters have an influence on the inverse design of runner blade. Their effects have been investigated through inverse computations under different given values of these parameters. When B_0 equals $0.425D_1$, $0.4D_1$ and $0.375D_1$, the velocity torque distribution in the span direction along the trailing edge of guide vane is shown in Figure 10 by circles, quadrilaterals and triangles, respectively. The distributions are nearly the same and so the value of B_0 has little influence on runner blade design. But when D_0 equals $1.25D_1$, $1.2D_1$ and $1.16D_1$, the velocity torque distribution along guide vane trailing edge becomes that shown in Figure 11 by circles, quadrilaterals and triangles, respectively. Thus, the gradient of velocity torque in the radial direction in the blade region is quite different. As the gradient of velocity torque in the radial

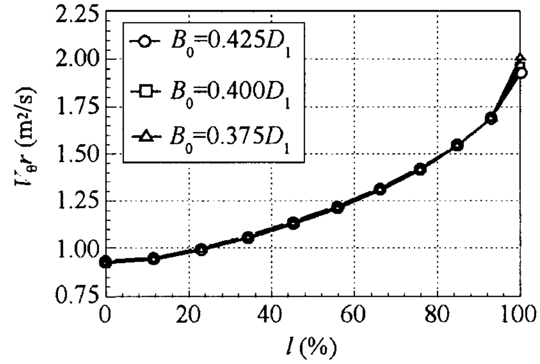

Figure 10. Velocity torque distribution along the trailing edge of guide vane (under different values of B_0).

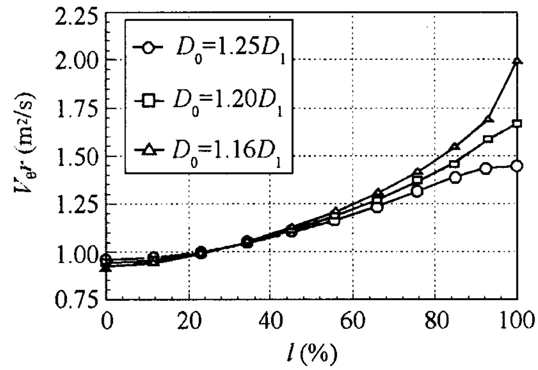

Figure 11. Velocity torque distribution along the trailing edge of guide vane (under different values of D_0).

direction has a great influence on the flow near the tip, a proper enlargement of guide vane distribution diameter D_0 is advantageous to improve runner blade twist. It is also beneficial to eliminate blade trailing vortex sheets and thereby to reduce the exit energy loss of the designed runner.

4. CONCLUSIONS

An improved Q3D inverse method has been proposed for hydraulic turbine blade design from the viewpoint of flow system. The computation domain is firstly taken from the far inlet of guide vane to the far outlet of runner blade in the inverse computation and the flow in different regions is solved simultaneously as a whole. So the influence of guide vane on runner blade design can be considered and the difficulty of defining the flow condition at the blade inlet is surmounted.

A set of rotational flow governing equations and a blade geometry design equation has been derived. As a pre-computation of initial blade design based on the S_{2m} stream surface is newly adopted, the iteration of S_1 and S_{2m} stream surface has been reduced greatly and the convergence of inverse computation has been improved. With this inverse model, it is convenient to control the performance of designed runner by adjusting the velocity torque distribution of design specification.

Experimental results and the direct flow analysis have verified the validity of the improved inverse model. Numerical investigation shows that a proper enlargement of guide vane distribution diameter is advantageous to improve the performance of axial flow hydraulic turbine runner to be designed. For its special features, the inverse method is easy to be applied into the comprehensive performance design optimization of axial hydraulic turbine runner.

REFERENCES

1. Schachenmann A, Muggli F, Gulich JF. Comparison of three-dimensional Navier–Stokes codes with LDA-measurements on an industrial radial pump impeller. In *Pump Machinery*, Cooper P (ed.). FED-vol. 154, ASME: New York, 1993; 231–236.
2. Schilling R, Ritzinger S. Numerical and experiment flow analysis in centrifugal pump impellers. *Proceedings of the JSME International Conference on Fluid Engineering*, Tokyo, 1997; 207–212.
3. Dulikeavich GS. Aerodynamic shape design and optimization: status and trends. *AIAA Journal of Aircraft* 1992; **29**(5):1020–1026.
4. Tan CS, Hawthorne WR, McCune JE, Wang C. Theory of blade design for large deflection: Part II-annular cascades. *ASME Transactions on Journal of Engineering for Gas Turbine and Power* 1984; **106**:354–365.
5. Borges JE. A three-dimensional inverse method for turbomachinery: Part-1 Theory. *ASME Transactions on Journal of Turbomachinery* 1994; **112**:346–354.
6. Xu JZ, Gu CW. A numerical procedure of three-dimensional design problem in turbomachinery. *ASME Transactions on Journal of Turbomachinery* 1992; **114**:548–582.
7. Zanetti L, Larocca F, Marsibio R. Euler solver for 3D inverse problems. *Proceedings of Advances and Applications in Computational Fluid Dynamics*, FED-vol. 66. ASME: New York, 1988; 71–79.
8. Zangeneh M, Goto A, Takemura T. Suppression of secondary flows in a mixed-flow pump impeller by application of three-dimensional inverse design method: Part 1—design and numerical validation. *ASME Transaction on Journal of Turbomachinery* 1996; **118**:536–543.
9. Peng G, Lin R. A Three-dimensional inverse method for the design of hydraulic runner with rotational coming flow. In *Fluid Machinery*, Roratgi US, Ogut A, Hayami H (eds), FED-vol. 222. ASME: New York, 1995; 161–166.
10. Wang QH, Zhu GX, Wu CH. Quasi-three dimensional and fully three-dimensional rotational flow calculation in turbomachines. *ASME Transactions on Journal of Engineering for Gas Turbine and Power* 1985; **107**: 227–285.
11. Lin R, Peng G. An advanced numerical simulation method for rotational flow in hydraulic turbomachinery. In *Fluid Machinery*, Roratgi US, Ogut A, Hayami H (eds), FED-vol. 222. ASME: New York, 1995; 173–176.
12. Rhie CM. Advanced transonic fan design procedure based on a Navier–Stokes method. *ASME Transaction on Journal of Turbomachinery* 1994; **116**:291–296.
13. Peng G, Cao S, Ishizuka M, Hayama S. Design optimization of axial flow hydraulic turbine runner Part II: multi-object constrained optimization method. *International Journal for Numerical Methods in Fluids* 2002; **39**.
14. Lin R. *Flow Dynamics Theory of Hydraulic Machinery*. Mechanical Industry Press: Beijing, 1996; 43–56 (in Chinese).
15. Peng G, Fujikawa S, Cao S, Lin R. An advanced three-dimensional inverse model for the design of hydraulic machinery runner. *Proceedings of the ASME/JSME Joint Fluid Engineering Conference* 1998, FED-vol. 245. New York, ASME: FEDSM98-4867.
16. Peng G, Cao S, Ishizuka M, Hayama S. Fully three-dimensional inverse computation of hydraulic impeller using finite element method. *Computational Fluid Dynamics Journal* 2001; **10**(2):247–254.
17. McFarland ER. A rapid blade-to-blade solution for use in turbomachinery design. *ASME Transaction, Journal of Engineering for Power* 1985; **100**:376–382.
18. Zangeneh M. A compressible three-dimensional design method for mixed and radial flow turbomachinery blades. *International Journal for Numerical Methods in Fluids* 1991; **13**:599–624.

